Journal of Engineering Mathematics **29:** 591–606, 1995.

Velocity inversion for acoustic waves with wavelet operator

SONG SHOUGEN and HE JISHAN
Central South University of Technology, Institute of Applied Geophysics, Hunan, Changsha, 410083, P.R. China

Received 9 February 1994; accepted in revised form 30 May 1995

Abstract. Seismic exploration is an important method in geophysical engineering. In this paper, with three-dimensional wavelet operator, a new inverse and imaging method is presented to the seismic inversion problem. Compared with the singular-function method in [1], [2] and [3], the method in this paper can suppress the noise in real-world data and can provide a formula to estimate the error produced by the band-limited nature of the data. As a result, the location of the interior surface in the earth can be detected more precisely.

1. Introduction

Bleistein and Cohen presented a theory for asymptotic inversion of observations for the acoustic wave equation in [1–3]. The inversion operator $\beta(x)$ was introduced by them and, by using velocity singularities, they have shown that $\beta(x)$ is a band-limited Delta function on the interior surface for the band-limited input data. Because the inversion operator $\beta(x)$ in [2–3] is a generalization of the derivative operator $\partial\alpha(z)/\partial z$ in [1], $\beta(x)$ is highly sensitive to noise in real-world data. On the other hand, the observed data are limited by the frequency band being used in seismic exploration and, in this case, the inversion operator $\beta(x)$ in [2–3], which is a band-limited Delta function on the interior surface, will produce error. How to estimate this is another matter. Therefore, it is necessary to find a new inversion method which can suppress the noise and can also analyse the error in the imaging process.

Recently, the subject of wavelet analysis has drawn a great deal of attention from mathematical scientists in various disciplines [4], [5] and [7]. It is creating a common link between mathematicians, physicists and engineers. In this paper, based on the approximate formulae developed by Bleistein, the authors advance a new method of velocity inversion by using the properties of the double localization in the space-frequency domain of the wavelet function as well as the focusing function. A theoretical analysis is made and the new imaging formulas are obtained.

Of course, it should be admitted that inverse problems are ill-posed. However, this is not the same for all inverse-problem methods. A general guiding rule is to ask only what you expect from the data. A simple example is to avoid trying to extract signal from a portion of the frequency band consisting only of or mostly of noise. With such simple considerations we extract the singularity of the velocity to map the interface in the earth by the wavelet operator. Fortunately, the techniques described in this paper are sufficiently robust that the quality of the results "degrade gracefully" when the ideal conditions are not met.

We will show that the method in this paper can not only suppress the noise in the observed data by the wavelet's focusing function, but also analyse the effect of the band-limited nature of the input data. Finally, we check it by numerical computation.

To emphasize the basic idea, here we consider only the seismic inverse problem for the constant background zero-offset case.

2. Wavelet operator and the recognition of interior surface

First, we introduce a right-handed coordinate system $x = (x_1, x_2, x_3)$ with x_3 being positive in the downward direction into the earth. The observed field is the back-scatter response from an acoustic point source set off at every point $\zeta = (\zeta_1, \zeta_2, 0)$ on the surface of the earth. We assume the total field $u(x, \zeta, \omega)$ is the solution of the three-dimensional Helmholtz equation with point source at $\zeta = (\zeta_1, \zeta_2, 0)$:

$$\nabla^2 u(x, \zeta, \omega) + \frac{\omega^2}{v^2} u(x, \zeta, \omega) = -\delta(x_1 - \zeta_1)\delta(x_2 - \zeta_2)\delta(x_3). \tag{2.1}$$

with the Sommerfeld's radiation conditions

ru is bounded,

$$r\left[\frac{\partial u}{\partial r} - \frac{\mathrm{i}\omega}{v} u\right] \to 0 \text{ as } r \to \infty,$$

where $v = |x|$, $v = v(x)$ is the wavespeed we seek.

The wavespeed is represented as a perturbation on a known reference speed, $c(x)$, expressed mathematically as follows:

$$\frac{1}{v^2(x)} = \frac{1}{c^2(x)}[1 + \alpha(x)]. \tag{2.2}$$

We decompose the total field into an incident and scattered field,

$$u(x, \zeta, \omega) = u_I(x, \zeta, \omega) + u_s(x, \zeta, \omega). \tag{2.3}$$

Similarly as Bleistein et al. [2], when the subsurface velocity variation is small, under Born approximation, for the constant background zero-offset case, one obtains

$$\begin{aligned} \alpha(x) = & \frac{8c_0^3}{i\pi^2} \int_{-\infty}^{\infty} \mathrm{d}^2\zeta \int_{-\infty}^{\infty} k_3 \exp\{2i[k \cdot (\rho - \zeta) - k_3 x_3]\} \, \mathrm{d}^3 k \\ & \times \frac{1}{\omega^2} \int_0^{\infty} t u_s(\zeta, \zeta, t) \exp\{i\omega t\} \left[1 + \frac{2i}{\omega t}\right] \mathrm{d}t. \end{aligned} \tag{2.4}$$

Where, $\mathrm{d}^2\zeta = \mathrm{d}\zeta_1 \mathrm{d}\zeta_2$, $d^3k = \mathrm{d}k_1 \mathrm{d}k_2 \mathrm{d}k_3$, $\rho = (x_1, x_2, 0)$, $\zeta = (\zeta_1, \zeta_2, 0)$, $k = (k_1, k_2, k_3)$, $\omega = c_0 \operatorname{sgn}(k_3) \cdot \sqrt{k_1^2 + k_2^2 + k_3^2}$.

Under the high-frequency assumption, from (2.4), one obtains

$$\begin{aligned} \alpha(x) = & \frac{8c_0^3}{i\pi^2} \int_{-\infty}^{\infty} \mathrm{d}^2\zeta \int_{-\infty}^{\infty} k_3 \exp\{k \cdot (\rho - \zeta) + k_3 x_3]\} \, \mathrm{d}^3 k \\ & \times \frac{1}{\omega^2} \int_0^{\infty} t u_s(\zeta, \zeta, t) \exp\{i\omega t\} \, \mathrm{d}t. \end{aligned} \tag{2.5}$$

There is a problem. When the subsurface velocity variation is not small and the observed data is band-limited in frequency and contains noise, how much information of the true unknown $\alpha(x)$ does the $\alpha(x)$ in equation (2.5) contain? That is unclear.

In this section we investigate the relation between the interior surface and the modulus maxima of the wavelet transform of $\alpha(x)$. We discover that, although $\alpha(x)$ in equation (2.5) is different from the true unknown function $\alpha(x)$, the singularities of $\alpha(x)$ in equation (2.5) are almost the same as the true unknown $\alpha(x)$ for a single interior surface.

Motivated by [4], we choose three-dimension wavelet functions $\psi^1(x)$, $\psi^2(x)$ and $\psi^3(x)$ as follows:

$$\psi^i(x) = \frac{\partial Q(x)}{\partial x_i}, \quad i = 1,2,3, \quad x = (x_1, x_2, x_3). \tag{2.6}$$

Where, $Q(x) = \dfrac{1}{2\pi\sqrt{2\pi}} \exp\left(-\dfrac{x_1^2 + x_2^2 + x_3^2}{2}\right)$ is the Gaussian function.

Let $Q_s(x) = \dfrac{1}{s^3} Q\left(\dfrac{x}{s}\right)$ and $\psi^i(x) = \dfrac{1}{s^3}\psi^i\left(\dfrac{x}{s}\right)$.

The wavelet transforms are given by,

$$W_s^i \alpha(x) = (\alpha * \psi_s^i)(x) = s\frac{\partial}{\partial x_i}(\alpha * Q_s)(x), \quad i = 1,2,3 \tag{2.7}$$

in which "$*$" is the convolution operator.

Under scale s, the three-dimension wavelet operator W is given by

$$W_s\alpha(x) = \begin{pmatrix} W_s^1\alpha(x) \\ W_s^2\alpha(x) \\ W_s^3\alpha(x) \end{pmatrix} = s \begin{pmatrix} \dfrac{\partial}{\partial x_1}(\alpha * Q_s)(x) \\ \dfrac{\partial}{\partial x_2}(\alpha * Q_s)(x) \\ \dfrac{\partial}{\partial x_3}(\alpha * Q_s)(x) \end{pmatrix} = s\nabla(\alpha * Q_s)(x), \tag{2.8}$$

where "∇" is the gradient operator.

By equation (2.8), we can prove that the modulus maxima of $W_s\alpha(x)$ are attained on the interior surface. Therefore, we know the location of the interior surface by detecting the maxima of $|W_s\alpha(x)|$.

In the following, we give the main results of this paper. The proof is given in Appendix A and B.

2.1. At the single tilted plane case

As is shown in Fig. 1, suppose the equation of tilted plane S is

$$x_1 \sin\theta\cos\varphi + x_2 \sin\theta \sin\varphi + x_3 \cos\theta - h\cos\theta = 0,$$

with speed $v = c_0$ above the plane and speed $v = c_1$ below the plane. Let $\zeta = (\zeta_1, \zeta_2, 0)$ be a point on the earth's surface. Suppose a unit impulse is set off at the surface, the reflected data observed at the surface can be approximated by

$$u_s(\zeta, t) = R\frac{\delta(t - 2l/c_0)}{8\pi l}. \tag{2.9}$$

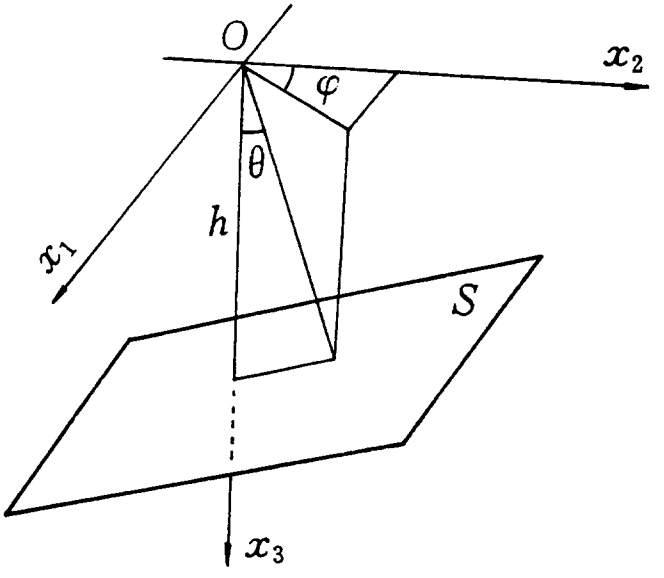

Fig. 1. Model for tilted plane.

Where, $l = h\cos\theta - \zeta_1\cos\varphi\sin\theta - \zeta - 2\sin\varphi\sin\theta$, R is the normal incidence reflection coefficient, which is,

$$R = \frac{c_1 - c_0}{c_1 + c_0}.$$

If the data $u_s(\zeta, t)$ are substituted in equation (2.5) and the calculations are carried out, one obtains

$$\alpha(x) = \frac{2R}{\pi}\int_{-\infty}^{\infty}\frac{1}{i\omega}\exp\{2i\omega[(-x_1\cos\varphi - x_2\sin\varphi)\sin\theta + (h - x_3)\cos\varphi]/c_0\}\,\mathrm{d}\omega. \tag{2.10}$$

Here $\omega = c_0 k_3 \sec\theta$.

Based on (2.8) and (2.10), we obtain

$$|W_s\alpha(x)| = \frac{2\sqrt{2}Rc_0}{\sqrt{\pi}}\exp\left\{-\frac{1}{2s^2}[(x_1\cos\varphi + x_2\sin\varphi)\sin\theta + (x_3 - h)\cos\theta]^2\right\}. \tag{2.11}$$

But, in practice, the frequency used is limited. So, ω in (2.10) varies not from $-\infty$ to ∞, but from ω_1 to ω_2, where $\omega_2 > \omega_1 > 0$. In this case, we have to analyse the effects of the limited bandwidth. In this paper the following results are obtained

$$|W_s\alpha(x)| = \frac{4Rs}{\pi}\exp\left\{-\frac{b^2}{4a}\right\}\left|\int_{\omega_1}^{\omega_2}\exp(-a\omega^2)\,\mathrm{d}\omega + Z(a, b, \omega_1, \omega_2)\right|. \tag{2.12}$$

Here

$$a = 2s^2/c_0^2, \qquad b = 2[(-x_1\cos\varphi - x_2\sin\varphi)\sin\theta + (h - x_3)\cos\theta]/c_0 \tag{2.13}$$

$$\left|\exp\left(-\frac{b^2}{4a}\right) Z(a,b,\omega_1,\omega_2)\right|$$
$$\leqslant \frac{1}{a}[\exp(-a\omega_1^2)+\exp(-a\omega_2^2)]\exp\left\{-\frac{1}{4a}(b^2-\tau_0^2)\right\} \tag{2.14}$$

in which $\tau_0 \in (0,b)$ or $\tau_0 \in (b,0)$, if $b=0$, $Z(a,b,\omega_1,\omega_2)=0$.

In (2.12) and (2.14), let $\omega_1 \to -\infty$ and $\omega_2 \to +\infty$. Then we obtain

$$\left|\exp\left(-\frac{b^2}{4a}\right) Z(a,b,\omega_1,\omega_2)\right| \to 0$$

and then, from (2.12)

$$|W_s\alpha(x)| = \frac{4Rs}{\pi}\exp\left(-\frac{b^2}{4a}\right)\int_{-\infty}^{\infty}\exp(-a\omega^2)\mathrm{d}\omega = \frac{4Rs}{\pi}\exp\left(-\frac{b^2}{4a}\right)\sqrt{\frac{\pi}{a}}$$
$$= \frac{2Rc_0\sqrt{2}}{\sqrt{\pi}}\exp\left\{-\frac{1}{2s^2}[(x_1\cos\varphi + x_2\sin\varphi)\sin\theta + (x_3-h)\cos\theta]^2\right\}.$$

This is the same as (2.11).

From (2.12), when $b=0$, that is,

$$(x_1\cos\varphi + x_2\sin\varphi)\sin\theta + (x_3-h)\cos\theta = 0,$$

the value of $|W_s\alpha(x)|$ is maximal.

Therefore, we can know the location of the interior surface by detecting the modulus maxima of $W_s\alpha(x)$.

2.2. THE GENERAL CASE

Suppose the equation of the interior surface S is $f(x_1,x_2,x_3)=0$, and for x close enough to the surface S there will be only one perpendicular from x to S. Suppose the normal vector of the surface S in $\bar{x}_0$ is $\hat{n}_0$, here $\hat{n}_0 = (f'_{x_1}(\bar{x}_0), f'_{x_2}(\bar{x}_0), f'_{x_3}(\bar{x}_0))$.

If x is near to surface S, we obtain the following result

$$|W_s\alpha(x)| \sim \frac{4Rs}{\sqrt{\pi}}\exp\left\{-\frac{b^2}{4a}\right\}\left|\int_{\omega_1}^{\omega_2}\exp(-a\omega^2)\,\mathrm{d}\omega + Z(a,b,\omega_1,\omega_2)\right| \tag{2.15}$$

in which

$$b = f'_{x_1}(\bar{x}_0)(x_1-\bar{x}_{01}) + f'_{x_2}(\bar{x}_0)(x_2-\bar{x}_{02}) + f'_{x_3}(\bar{x}_0)(x_3-\bar{x}_{03}), \tag{2.16}$$

$$a = 2s[f'^2_{x_1}(\bar{x}_0) + f'^2_{x_2}(\bar{x}_0) + f'^2_{x_3}(\bar{x}_0)]\mu^2\omega^2/c_0^2, \tag{2.17}$$

where $Z(a,b,\omega_1,\omega_2)$ satisfies $Z(a,b,\omega_1,\omega_2)=0$ as $b=0$, and

$$\left|\exp\left(-\frac{b^2}{4a}\right) Z(a,b,\omega_1,\omega_2)\right| \leqslant \frac{1}{a}[\exp(-a\omega_1^2)+\exp(-a\omega_2^2)]\exp\left[-\frac{1}{4a}(b^2-\tau_0^2)\right]. \tag{2.18}$$

Particularly, if x is on the surface S, then the value of $|W_s\alpha(x)|$ is maximal:

$$|W_s\alpha(x)| \sim \frac{4Rs}{\sqrt{\pi}} \int_{\omega_1}^{\omega_2} \exp(-a\omega^2)\,\mathrm{d}\omega. \tag{2.19}$$

Comparing with the inverstion operator $\beta(x)$ introduced in [2] and [3], from (2.15), (2.18) and (2.19), we can not only detect the location of the interior surface more precisely but also estimate the effect of band-limited nature of the input data. This result will be checked by numerical computation in section 4.

3. The analysis of the effects of the noise in data

Because there always exists noise in the observed data, it is important to find the velocity-inversion method which can suppress the noise. To emphasize the basic idea, our work is performed only for the one-dimensional case.

In the one-dimensional case, an impulsive source, $-\delta(x_3 - x_{s3})$, is assumed to act at depth x_{s3} (the source position), and at time $t = 0$. Similar to (2.5) for the constant background zero-offset case, one obtains

$$\alpha(x_3) = -\frac{4}{\pi c_0} \int_{-\infty}^{\infty} u_s(0,0,\omega)\, \mathrm{e}^{-2i\omega x_3/c_0}\,\mathrm{d}\omega. \tag{3.1}$$

Suppose that $u_s(0,0,\omega)$ is affected by $n(\omega)$ and the observed data becomes $u_s(0,0,\omega) + n(\omega)$, where $n(\omega)$ is the Fourier transform of the noise $n(t)$. Then, $\alpha(x_3)$ correspondingly becomes $\bar{\alpha}(x_3)$, such that

$$\bar{\alpha}(x_3) = \alpha(x_3) - \frac{4}{\pi c_0} \int_{-\infty}^{\infty} n(\omega)\, \mathrm{e}^{-2i\omega x_3/c_0}\,\mathrm{d}\omega. \tag{3.2}$$

That is

$$\bar{\alpha}(x_3) = \alpha(x_3) - 2n(x_3). \tag{3.3}$$

Equation (3.3) implies that the noise in the observed data should affect the $\alpha(x_3)$.

If we let the wavelet operator W act on the equation (3.3), we obtain

$$W_s\bar{\alpha}(x_3) = W_s\alpha(x_3) - 2W_sn(x_3). \tag{3.4}$$

Suppose the noise $n(x_3)$ is real wide-sense stationary white noise of variance σ^2. We denote by $E(X)$ the expected value of a random variable x. In this paper the wavelet $\psi(x)$ is real. Grossmann et al. in [5] have shown that the decay of $E(|W_sn(x_3)|^2)$ is proportional to $1/s$.

On the other hand, Mallat *et al.* in [4] have shown that the Lipschitz exponent γ of step function $\alpha(x)$ is equal to zero and the Lipschitz exponent γ of white noise $n(x_3)$ is equal to $-\frac{1}{2} - \varepsilon$, for $\varepsilon > 0$.

Furthermore, Mallat et al. in [4] have shown that if a tempered distribution $f(x)$ has a uniform Lipschitz exponent γ, there exists constant K such that

$$|W_sf(x)| \leqslant Ks^{\gamma}. \tag{3.5}$$

Therefore, by the above discussion, we know that there exist two constants k_0 and k_1 such that

$$|W_s\alpha(x_3)| \leqslant k_0 \tag{3.6}$$

and

$$|W_s n(x_3)| \leqslant k_1 s^{-\frac{1}{2}-\varepsilon}. \tag{3.7}$$

The equations (3.6) and (3.7) imply that the modulus maxima of the wavelet transform of the noise $n(x_3)$ should decrease (or increase) when the scale increases (or decreases), but, the modulus maxima of the wavelet transform of $\alpha(x_3)$ should remain constant over a large range of scales.

In fact, by the equations (2.11) and (2.15), we can obtain the same result, that is, the modulus maxima of $W_s\alpha(x_3)$ remain constant or increase when the scale s increases.

So, when scale s is positive and smaller than 1, $\bar{\alpha}(x_3)$ is dominated by the noise and it is extremely difficult to recover any position information of interior surface from the maxima of $|W_s\bar{\alpha}(x_3)|$. But when the scale increases and becomes larger than 1, the maxima of $|W_s n(x_3)|$ become much smaller, which means that the effects of noise become weaker and weaker. At this moment, the $\bar{\alpha}(x_3)$ in equation (3.3) is dominated by the $\alpha(x_3)$ and it is very easy to know the position of the interior surface from the maxima of $|W_s\bar{\alpha}(x_3)|$.

4. Numerical check

4.1. Computer implementation

We now simply describe the numerical procedure to calculate the $W_s\alpha(x)$.

(1) Using Fourier Transform and the inverse Fourier Transform in three variables, we can carry out the calculations of $\alpha(x)$ from the observed data $u_s(\zeta, t)$. The details of the calculation can be found, for instance, in [2].

(2) Using discrete fast wavelet transform, which can be found, for instance, in [4] and [7], $W_s\alpha(x)$ can be calculated.

(3) Choose the maximal value of $|W_s\alpha(x)|$ to determine the location of the reflector.

4.2. Numerical examples

For the band-limited input data, to check the imaging formula in this paper, let us consider a single inclined planar reflector. The angle of inclination is 30 degrees with respect to a horizontal ox_1 axis, and the planar reflector is parallel to ox_2 axis, that is $\theta = 30°$ and $\phi = 0°$ in Fig. 1. Above the plane, the speed $c_0 = 4500$ m/sec, and below the plane, the speed $c_1 = 5500$ m/sec. The inclined plane is assumed to be at depth 2000 m below the original point $(0, 0, 0)$.

Fig. 2 shows that the image of the reflector produced by $|W_s\alpha(x)|$ is correct. On the other hand, comparing with the results in [1], [2] and [3], we know that, although the location of the reflector can be detected correctly by two inverse operators $W_s\alpha(x)$ in this paper and $\beta(x)$ in [2], for the input data not containing any noise, our inverse method can estimate the effect produced by the band-limited nature of the input data (see the equations (2.15) and (2.18) in this paper).

For the same theory model in Fig. 2, we add the real white noise to the data $u_s(\zeta, \zeta, t)$ (the SNR is 3.4 dB). The image produced by the inverse operator $\beta(x)$ introduced in [2] is shown

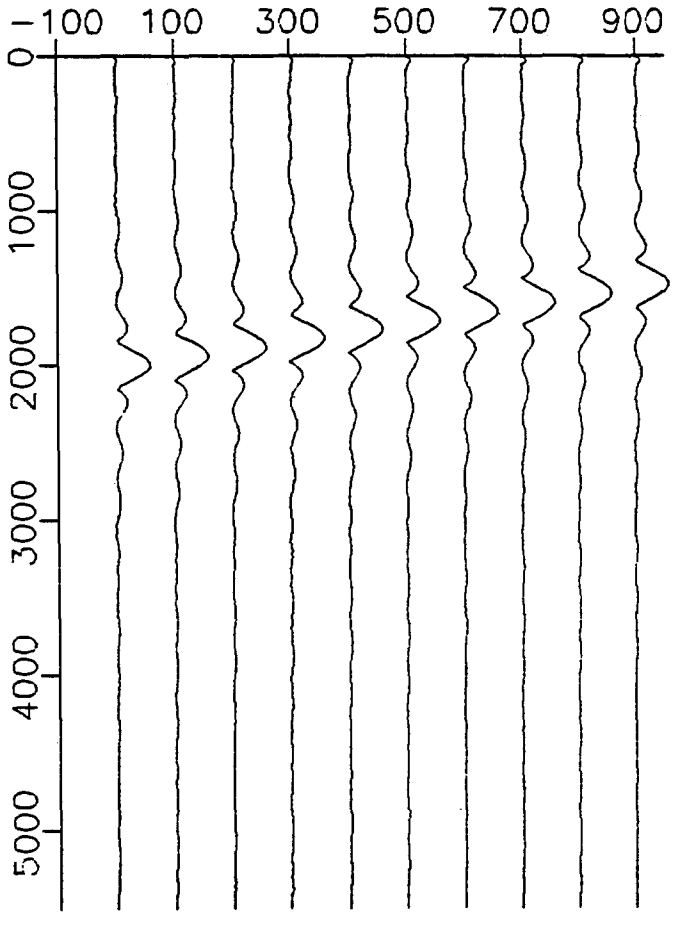

Fig. 2. A 6–50 Hz bandwidth representation of $|W_s\alpha(x)|$, scale $s = 2^1$.

in Fig. 3. The effects of the noise to $\beta(x)$ is very serious, and we can not know where the location of the planar reflector is and how many the reflectors there exist.

But, in Fig. 4, the image of the same reflector produced by the modulus maxima of $W_s\alpha(x)$ is far more desirable. Calculations show that $W_s\alpha(x)$ can suppress noise very well as the scale s being larger than 2^3. But the scale s should stay in a suitable range, for example, s smaller than 2^8, because some spatial resolution may be lost for too large a scale.

In Fig. 3, the SNR is 0.8 dB. In Fig. 4(a), (b) and (c), the SNR is 2.2 dB, 6.4 dB and 16.8 dB respectively.

5. Discussion of results

In this paper, based on the approximate formulas developed by Bleistein, the authors advanced a new method of velocity inversion. Using the property of the localization in space domain of the wavelet, we showed that the singularity of the velocity can be extracted and characterised from the local maxima of the wavelet operator. In this paper, the new image formulas are obtained. Based on these formulas (eq. (2.15), (2.18) and (2.19)), we can not only detect the location of the reflector in the earth, but also estimate the effect of the band-limited nature of the input data. Through the theoretical analysis and numerical check, we showed that

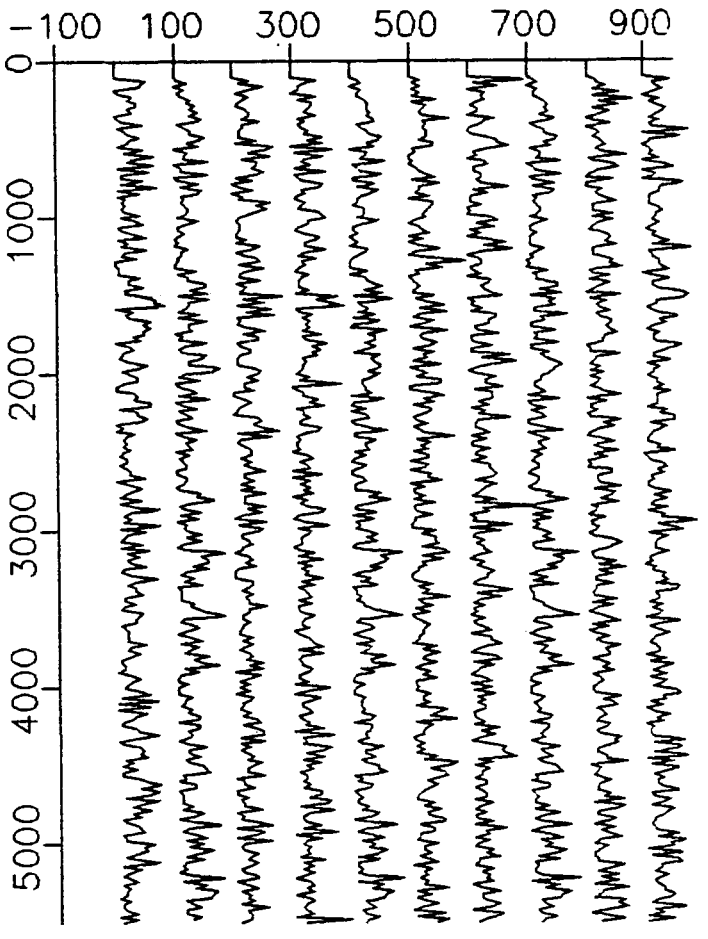

Fig. 3. Adding real white noise to input data, a 6–50 Hz bandwidth depth section determined by $\beta(x)$.

our method can suppress the noise in the observed data and can estimate the effect of the band-limited input data.

In this paper, we only deal with the imaging problem in a constant background. The inversion in the variable media will be considered in another paper.

6. Appendix A

First let us give the proof of eq. (2.11). We apply the wavelet operator (2.8) to $\alpha(x)$ in (2.10). To calculate $W_s\alpha(x)$, we need to calculate $W_s^j\alpha(x)$, $j = 1, 2, 3$. By eq. (2.7), we obtain

$$\begin{aligned} W_s^1\alpha(x) \;=\; & -\frac{2Rs}{\pi^2\sqrt{2\pi}}\cos\varphi\sin\theta\int_{-\infty}^{\infty}d\omega\int_{-\infty}^{\infty}\exp\{2i\omega[((y_1-x_1)\cos\varphi \\ & +(y_2-x_2)\sin\varphi)\sin\theta+(h+y_3-x_3)\cos\theta]/c_0\} \\ & \times\frac{1}{s^3}\exp\left(-\frac{y_1^2+y_2^2+y_3^2}{2s^2}\right)dy_1\,dy_2\,dy_3. \end{aligned} \tag{A.1}$$

By using the formula

$$\int_{-\infty}^{\infty}\exp(i\omega x-x^2/2)\,dx=(2\pi)^{1/2}\exp(-\omega^2/2)$$

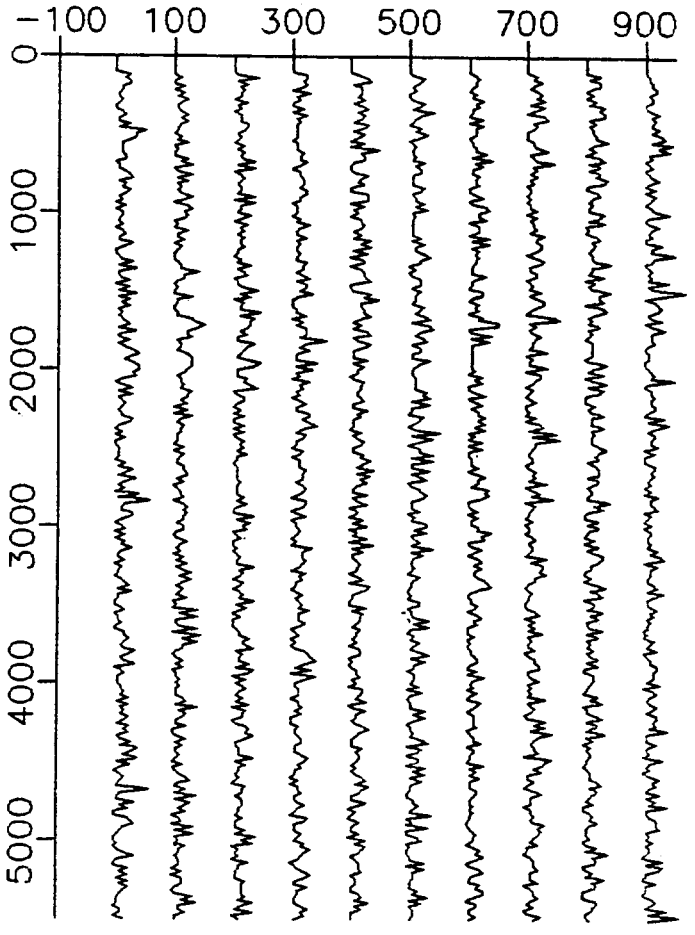

Fig. 4. (a)

we get

$$W_s^1\alpha(x) = -\frac{2\sqrt{2}Rc_0}{\sqrt{\pi}}\cos\varphi\sin\theta\int_{-\infty}^{\infty}\exp\left(-\frac{2s^2}{c_0^2}\omega^2 + ib\omega\right)\mathrm{d}\omega, \tag{A.2}$$

in which,

$$a = 2s^2/c_0^2 \quad \text{and} \quad b = 2[(-x_1\cos\varphi - x_2\sin\varphi)\sin\theta + (h - x_3)\cos\varphi]/c_0.$$

Due to

$$\int_{-\infty}^{\infty}\exp(-a\omega^2)\sin b\omega\,\mathrm{d}\omega = 0, \qquad \int_{-\infty}^{\infty}\exp(-a\omega^2)\cos b\omega\,\mathrm{d}\omega = \sqrt{\frac{\pi}{a}}\exp\left(-\frac{b^2}{4a}\right),$$

we find

$$W_s^1\alpha(x) = -\frac{2\sqrt{2}Rc_0}{\sqrt{\pi}}\cos\varphi\sin\theta \times \exp\left\{-\frac{1}{2s^2}[(x_1\cos\varphi + x_2\sin\varphi)\sin\theta + (x_3 - h)\cos\theta]^2\right\}. \tag{A.3}$$

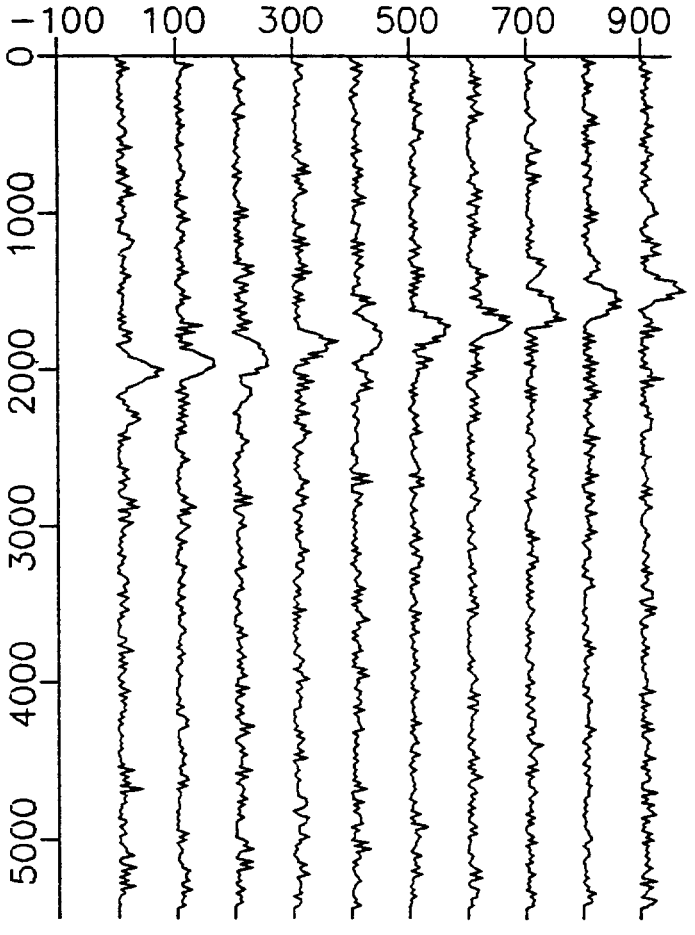

Fig. 4. (b)

Similarly, the calculations of $W_s^2\alpha(x)$ and $W_s^3\alpha(x)$ are carried out and we obtain

$$W_s^2\alpha(x) = -\frac{2\sqrt{2}Rc_0}{\sqrt{\pi}}\sin\varphi\sin\theta \times \exp\left\{-\frac{1}{2s^2}[(x_1\cos\varphi + x_2\sin\varphi)\sin\theta + (x_3 - h)\cos\theta]^2\right\} \tag{A.4}$$

and

$$W_s^3\alpha(x) = -\frac{2\sqrt{2}Rc_0}{\sqrt{\pi}}\cos\theta \times \exp\left\{-\frac{1}{2s^2}[(x_1\cos\varphi + x_2\sin\varphi)\sin\theta + (x_3 - h)\cos\theta]^2\right\}. \tag{A.5}$$

Note that, $|W_s\alpha(x)| = \sqrt{|W_s^1\alpha(x)|^2 + |W_s^2\alpha(x)|^2 + |W_s^3\alpha(x)|^2}$ and $\cos^2\varphi\sin^2\theta + \sin^2\varphi\sin^2\theta + \cos^2\theta = 1$, so that

$$|W_s\alpha(x)| = -\frac{2\sqrt{2}Rc_0}{\sqrt{\pi}}\exp\left\{-\frac{1}{2s^2}[(x_1\cos\varphi + x_2\sin\varphi)\sin\theta + (x_3 - h)\cos\theta]^2\right\}. \tag{A.6}$$

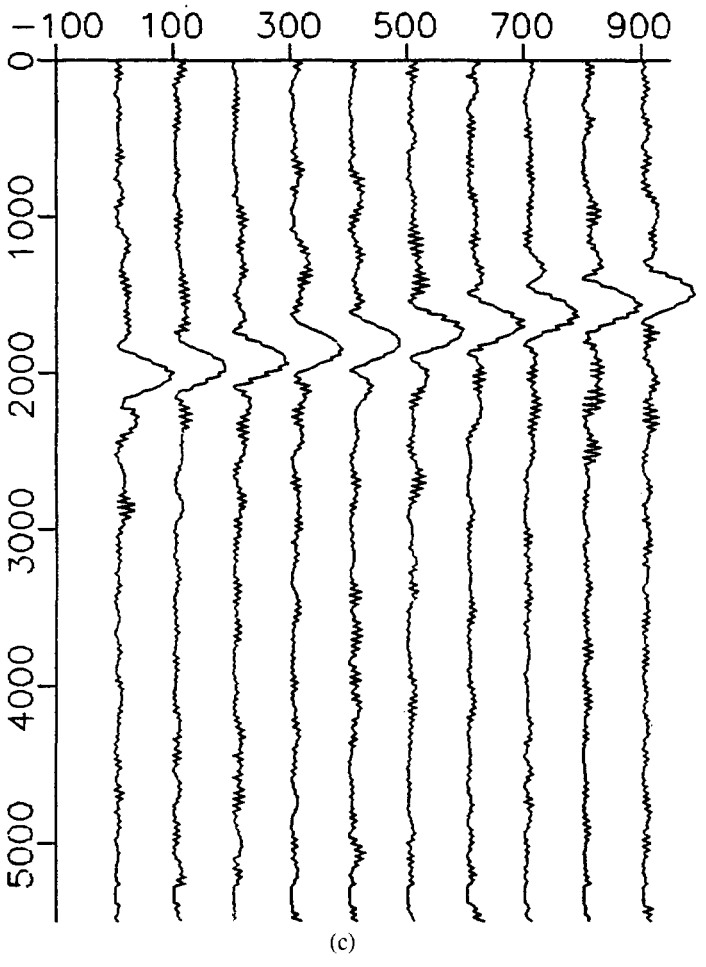

Fig. 4. (a)–(c) Adding real white noise to input data, a 6–50 Hz bandwidth depth section determined by $|W_s\bar{\alpha}(x)|$ under scales s taking 2^0, 2^1 and 2^3, respectively.

Equation (A.6) completes the proof of eq. (2.11).

Now, let us prove eq. (2.12). For the case of limited bandwith, equation (A.2) becomes

$$W_s^1\alpha(x) = -\frac{2Rs\cos\varphi\sin\theta}{\pi^2\sqrt{2\pi}}[z_1(b) + iz_2(b)]. \tag{A.7}$$

Where,

$$z_1(b) = \int_{\omega_1}^{\omega_2} \exp(-a\omega^2)\cos b\omega\,\mathrm{d}\omega, \quad z_2(b) = \int_{\omega_1}^{\omega_2} \exp(-a\omega^2)\sin b\omega\,\mathrm{d}\omega, \tag{A.8}$$

in which,

$$a = \frac{2s^2}{c_0^2}, \qquad b = \frac{2[(-x_1\cos\varphi - x_2\sin\varphi)\sin\theta + (h - x_3)\cos\theta]}{c_0}.$$

Due to

$$\begin{cases} \dfrac{\mathrm{d}z_1(b)}{\mathrm{d}b} = -\dfrac{b}{2a}z_1(b) + \dfrac{1}{2a}[\exp(-a\omega_2^2)\sin b\omega_2 - \exp(-a\omega_1^2)\sin b\omega_1], \\ \dfrac{\mathrm{d}z_2(b)}{\mathrm{d}b} = -\dfrac{b}{2a}z_2(b) + \dfrac{1}{2a}[\exp(-a\omega_2^2)\cos b\omega_2 - \exp(-a\omega_1^2)\cos b\omega_1], \end{cases}$$

we obtain

$$z_1(b) = \exp\left(-\frac{b^2}{4a}\right)\left[\int_{\omega_1}^{\omega_2}\exp(-a\omega^2)\,\mathrm{d}\omega + \int_0^b(\exp(-a\omega_2^2)\sin b\omega_2 - \exp(-a\omega_1^2)\sin b\omega_1)\frac{1}{2a}\exp\left(\frac{b^2}{4a}\right)\mathrm{d}b\right], \tag{A.9}$$

$$z_2(b) = -\exp\left(-\frac{b^2}{4a}\right)\left[\int_0^b(\exp(-a\omega_2^2)\cos b\omega_2 - \exp(-a\omega_1^2)\cos b\omega_1)\frac{1}{2a}\exp\left(\frac{b^2}{4a}\right)\mathrm{d}b\right]. \tag{A.10}$$

From (A.7), (A.9) and (A.10), we have

$$W_s^1\alpha(x) = -\frac{4Rs\cos\varphi\sin\theta}{\pi} \times\left[\exp\left(-\frac{b^2}{4a}\right)\int_{\omega_1}^{\omega_2}\exp(-a\omega^2)\,\mathrm{d}\omega + \exp\left(-\frac{b^2}{4a}\right)Z(a,b,\omega_1,\omega_2)\right]. \tag{A.11}$$

Where,

$$Z(a,b,\omega_1,\omega_2) = \left\{\int_0^b\frac{1}{2a}\left[\exp(-a\omega_2^2)\sin b\omega_2 - \exp(-a\omega_1^2)\sin b\omega_1\right]\exp\left(\frac{b^2}{4a}\right)\mathrm{d}b - i\int_0^b\frac{1}{2a}\left[\exp(-a\omega_2^2)\cos b\omega_2 - \exp(-a\omega_1^2)\cos b\omega_1\right]\exp\left(\frac{b^2}{4a}\right)\mathrm{d}b\right\}. \tag{A.12}$$

Similarly, we obtain

$$W_s^2\alpha(x) = -\frac{4Rs\sin\varphi\sin\theta}{\pi} \times\left[\exp\left(-\frac{b^2}{4a}\right)\int_{\omega_1}^{\omega_2}\exp(-a\omega^2)\,\mathrm{d}\omega + \exp\left(-\frac{b^2}{4a}\right)Z(a,b,\omega_1,\omega_2)\right], \tag{A.13}$$

$$W_s^3\alpha(x) = -\frac{4Rs\cos\theta}{\pi} \times\left[\exp\left(-\frac{b^2}{4a}\right)\int_{\omega_1}^{\omega_2}\exp(-a\omega^2)\,\mathrm{d}\omega + \exp\left(-\frac{b^2}{4a}\right)Z(a,b,\omega_1,\omega_2)\right]. \tag{A.14}$$

Therefore

$$|W_s\alpha(x)| = \frac{4Rs}{\pi}\exp\left(-\frac{b^2}{4a}\right)\left|\int_{\omega_1}^{\omega_2}\exp(-a\omega^2)\,\mathrm{d}\omega + Z(a,b,\omega_1,\omega_2)\right|. \tag{A.15}$$

(A.12) and (A.15) complete the proof of eq. (2.14) and (2.12).

Appendix B

From (2.5), by the method of stationary phase which is found, for instance, in [6], we have

$$\alpha(x) = -\frac{16x_3}{\pi c_0}\int_\Sigma \frac{\mathrm{d}^2\zeta}{r}\int_{\omega_1}^{\omega_2} \mathrm{e}^{-2i\omega r/c_0} u_s(\zeta,\omega)\,\mathrm{d}\omega, \tag{B.1}$$

where $u_s(\zeta,\omega) = \int_0^\infty u_s(\zeta,t)\mathrm{e}^{i\omega t}\,\mathrm{d}t$, $r = \sqrt{(x_1-\zeta_1)^2+(x_2-\zeta_2)^2+x_3^2}$, Σ represents the total domain of recording positions ζ on the surface of the earth and (ω_1,ω_2) represents the k-domain corresponding to the band-limited range of ω.

For $u_s(\zeta,\omega)$ we use the Kirchoff approximation back-scattered field which can be found in [6],

$$u_s(\zeta,\omega) = \frac{i\omega}{8\pi^2 c_0}\int_S R\frac{\hat{n}\cdot\hat{r}_0}{r_0^2}\exp(2i\omega r_0/c_0)\,\mathrm{d}S, \tag{B.2}$$

where n is the unit upward normal vector, r_0 is a unit vector from the surface S to the observation point, $r_0 = |x_0-\zeta| = \sqrt{(x_{01}-\zeta_1)^2+(x_{02}-\zeta_2)^2+(x_{03}-\zeta_3)^2}$,

$$R = \frac{|\hat{n}\cdot\hat{r}_0|/c_0 - \sqrt{c_1^{-2}-c_0^{-2}+c_0^{-2}(\hat{n}\cdot\hat{r}_0)^2}}{|\hat{n}\cdot\hat{r}_0|/c_0 + \sqrt{c_1^{-2}-c_0^{-2}+c_0^{-2}(\hat{n}\cdot\hat{r}_0)^2}}$$

and the surface S is described in terms of two parameters, $(\sigma_1,\sigma_2) = \sigma$ with $x_0 = x_0(\sigma)$.

Note that $\mathrm{d}S = \sqrt{g}\,\mathrm{d}\sigma_1\,\mathrm{d}\sigma_2 = \sqrt{g}\,\mathrm{d}^2\sigma$. From (B.1) and (B.2) we obtain

$$\alpha(x) = \frac{2x_3 i}{\pi^3 c_0^2}\int_{\omega_1}^{\omega_2}\omega\,\mathrm{d}\omega\int_\Sigma\frac{\mathrm{d}^2\zeta}{r}\int_S\sqrt{g}\frac{\hat{n}\cdot\hat{r}_0}{r_0^2}R\exp\{2i\omega(r_0-r)/c_0\}\,\mathrm{d}^2\sigma, \tag{B.3}$$

where $g = \left|\dfrac{\partial x_0}{\partial\sigma_1}\times\dfrac{\partial x_0}{\partial\sigma_2}\right|^2 = \left|\det\left[\dfrac{\partial x_0}{\partial\sigma_j}\cdot\dfrac{\partial x_0}{\partial\sigma_k}\right]\right|, \qquad (j,k=1,2).$

In Fig. 5, given a point x close enough to the surface S, drop perpendiculars from x to S and $\bar{x}_0$ is the foot of the perpendicular. Each such perpendicular defines a possible value of σ at a stationary point. Extend each normal up to the data surface, ζ. For each ζ in the aperture Σ, the pair ζ, σ is a stationary point of the four-fold integral (B.3).

Let

$$\Phi(\zeta,\sigma) = r_0 - r. \tag{B.4}$$

Because the vectors, $\bar{x}_0-\zeta$ and $x-\zeta$ are colinear, the difference of distance defining Φ in (B.4) reduces to distance along the normal through x.

That is

$$\Phi = r_0 - r = d \tag{B.5}$$

with $d>0$ when x is above S and $d<0$ when x is below S measuring signed distance from S along the normal.

Applying the method of stationary phase to (B.3) we find

$$\alpha(x) = -\frac{2x_3\sqrt{g}R_n i}{\pi r r_0^2\sqrt{D}}\int_{\omega_1}^{\omega_2}\frac{1}{\omega}\exp\{2i\omega d/c_0\}\,\mathrm{d}\omega. \tag{B.6}$$

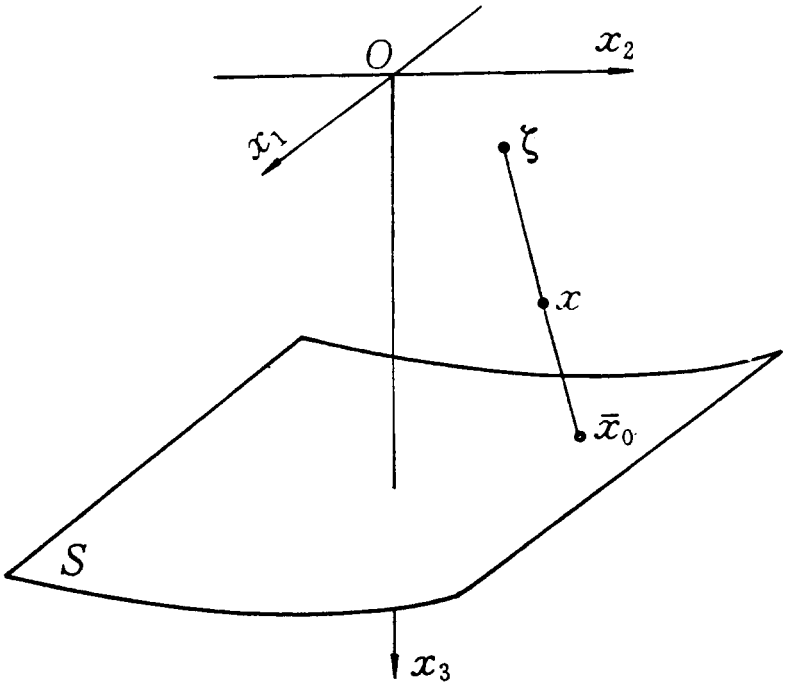

Fig. 5. Model for curved surface.

Where $D = |\det[\Phi_{ij}]|$, $[\Phi_{ij}] = \begin{bmatrix} \dfrac{\partial^2\Phi}{\partial\zeta_i\partial\zeta_j} & \dfrac{\partial^2\Phi}{\partial\zeta_i\partial\sigma_j} \\ \dfrac{\partial^2\Phi}{\partial\sigma_i\partial\zeta_j} & \dfrac{\partial^2\Phi}{\partial\sigma_i\partial\sigma_j} \end{bmatrix}$, $R_n = \dfrac{c_1 - c_0}{c_1 + c_0}$.

Especially, when x is on the surface S, we can carry out the calculation of $D = |\det[\Phi_{ij}]|$ and obtain $D = (gx_3^2)/(r_0^4 r^2)$.

Suppose the normal vector of surface S in $\bar{x}_0$ is $\hat{n}_0$, then $\hat{n} = (f'_{x_1}(\bar{x}_0), f'_{x_2}(\bar{x}_0), f'_{x_3}(\bar{x}_0))$. By (B.5), we know that there exists a factor $\mu > 0$ such that

$$d = \mu[f'_{x_1}(\bar{x}_0)(x_1 - \bar{x}_{01}) + f'_{x_2}(\bar{x}_0)(x_2 - \bar{x}_{02}) + f'_{x_3}(\bar{x}_0)(x_3 - \bar{x}_{03})] \tag{B.7}$$

From (B.6) and (B.7), we have

$$\begin{aligned}\alpha(x) = {} & \frac{2x_3\sqrt{g}R_n}{\pi r r_0^2\sqrt{D}} \int_{\omega_1}^{\omega_2} \frac{1}{i\omega} \exp\{2i\omega\mu[f'_{x_1}(\bar{x}_0)(x_1 - \bar{x}_{01}) + f'_{x_2}(\bar{x}_0)(x_2 - \bar{x}_{02}) \\ & + f'_{x_3}(\bar{x}_0)(x_3 - \bar{x}_{03})]/c_0\}\, d\omega.\end{aligned} \tag{B.8}$$

Now let us define

$$\begin{aligned}\alpha_1(x) = {} & \int_{\omega_1}^{\omega_2} \frac{1}{i\omega} \exp\{2i\omega\mu[f'_{x_1}(\bar{x}_{01})(x_1 - \bar{x}_{01}) + f'_{x_2}(\bar{x}_0)(x_2 - \bar{x}_{02}) \\ & + f'_{x_3}(\bar{x}_0)(x_3 - \bar{x}_{03})]/c_0\}\, d\omega\end{aligned}$$

If x is on the surface S, the coefficient of $\alpha(x)$ in (B.8) becomes $2R_n/\pi$, and when x is near to surface S, we know that $\alpha(x)$ is equal to $\alpha_1(x)$ multiplied by "a slowly varying function". Therefore, we have the following approximate formula

$$\alpha(x) \approx \frac{2R_n}{\pi}\alpha_1(x), \qquad \text{as } x \text{ near enough to surface } S. \tag{B.9}$$

Very similar to the proof of eq. (A.15), based on eq. (B.9) we can easily complete the proof of eq. (2.15).

Acknowledgements

This work was supported by IET foundation for the young teacher. The authors would like to thank S. Mallat for his help and advice. This paper is motivated by Bleistein's lecture (1992) in Shandong University of P.R. China.

References

1. J.K. Cohen and N. Bleistein, Velocity inversion procedure for acoustic waves. *Geophysics* 44 (1979) 1077–1087.
2. N. Bleistein, J.K. Cohen and F.G. Hagin, Computational and asymptotic aspects of velocity inversion. *Geophysics* 50 (1985) 1253–1265.
3. N. Bleistein, On the imaging of reflecting in the earth. *Geophysics* 52 (1987) 931–942.
4. S. Mallat and W.L. Hwang, Singularity detection and processing with wavelets. *IEEE Trans. On information theory* 38 (1992) 617–643.
5. A. Grossman, Wavelet transform and edge detection, in stochastic processes in physics and engineering, ed. M. Hazewinkel, Dordrecht, Reidel (1986).
6. N. Bleistein, Mathematical methods for wave phenomena. New York, Academic Press Inc. (1984).
7. C.K. Chui, Wavelets: A tutorial in theory and applications. Academic Press, inc., Boston, Harcourt Brace Jovanovich Publishers (1992).